# 2

# The Role of Functional Lung Imaging in the Improvement of Pulmonary Drug Delivery

*Andreas Fouras*[*] *and Stephen Dubsky*
*Department of Mechanical and Aerospace Engineering, Faculty of Engineering, Monash University, Australia*

## Abbreviations

**List of Abbreviations**

| | |
|---|---|
| CT | Computed tomography |
| 4DCT | Four-dimensional computed tomography |
| DNA | Deoxyribonucleic acid |
| EIT | Electrical impedance tomography |
| MRI | Magnetic resonance imaging |
| PBI | Propagation-based imaging |
| PET | Positron emission tomography |
| RF | Radio frequency |
| SPECT | Single photon emission computed tomography |

## 2.1 Introduction

It is well established that the distribution of pharmacological treatments delivered via inhalation into the respiratory system is heavily influenced by local variations in the flow of air within the lung and the topology of the airway tree. Additionally, delivery of pharmacological agents to the respiratory system will affect both the function and structure of the lung. For example, delivery of salbutamol

[*] Email: Andreas.Fouras@monash.edu

*Pulmonary Drug Delivery: Advances and Challenges*, First Edition. Edited by Ali Nokhodchi and Gary P. Martin.

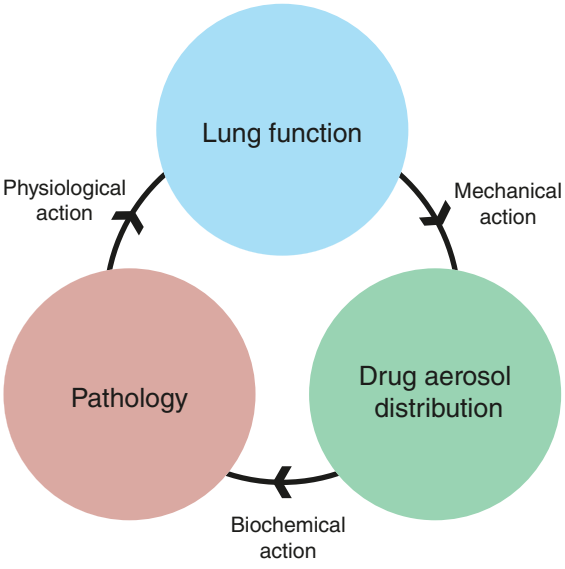


***Figure 2.1*** *The pulmonary drug delivery cycle*

causes bronchial dilation with subsequent increases in the peak flow and alterations in the flow distribution.

It is clear, therefore, that lung function plays a pivotal role in the process of pulmonary drug delivery (Figure 2.1). Currently, imaging is used to improve the speed and quality of decision making, and it can provide efficacy biomarkers and a better understanding of preclinical pharmacology [1]. The capacity of imaging lung function would extend the use of imaging in drug development even further by providing the direct measurement of a treatment's effect on lung function. Additionally, numerical models which provide uniquely useful data on deposition of inhaled treatments can be dramatically improved through the use of functional inputs and can, therefore, provide more accurate simulation outputs.

Here we demonstrate that functional lung imaging can

- aid the development of pulmonary drug delivery methods,
- offer the potential to be a major influence on the treatment, through customization of treatment parameters (dosage, particle size, etc.) for a patient's specific functional status, and
- be of use in monitoring the effects of treatment and disease progression.

The mechanical properties of an aerosol combined with the structure and flow of air through the lung produce a heterogeneous distribution of the aerosol. Subsequently, the action of the pharmaceutical impacts upon the pathology, which in turn affects lung function.

### 2.1.1 Particle Deposition

The distribution within the lung of an inhaled treatment agent has a large influence on the effectiveness of that treatment. Furthermore, during the drug development process, it is important to separate the effect of the delivery mechanism from the pharmacological action to accurately assess

its suitability. An otherwise viable treatment might not be effective if the drug is not delivered to the diseased area or site of desired action within the lung. Hence, treatment compounds of an excellent therapeutic value may be understood to have a lower value or even be completely discarded because of a lack of understanding of the complex interaction between aerosol deposition, lung pathology, and local or regional lung function.

Optimization of pulmonary drug delivery deposition presents many challenges. A particle's physical characteristics, including size and density, along with the airflow throughout the lung, determine its final deposition location. The airflow varies both temporally and spatially, and is determined by the geometry of the lung, the mechanical properties of the lung tissue (compliance and resistance), and the driving pressures within the lung, produced by the diaphragm and intercostal muscles. The challenge lies in the fact that these influences are very difficult to measure *in vivo*, and that all lung diseases will alter these factors. Furthermore, the particle deposition distribution is difficult to determine in a noninvasive manner. Consequently, both the causes and effects of the deposition mechanisms are hidden under real conditions. This has resulted in a limited understanding of the influence of various parameters on the particles' deposition and distribution in clinical situations.

The most widely used experimental method for measuring regional particle deposition has been nuclear medical imaging, whereby a radionuclide contrast agent is inhaled into the lung, and the radiation emitted from this agent is imaged to allow the measurement of its local concentration [2]. This provides a regional measurement of deposition; however, spatial resolution is not sufficient to correlate deposition with specific airway locations. Therefore, the potential to investigate the fundamental mechanisms of drug deposition using this method is limited.

A lack of experimental data has necessitated a focus on computer simulation of deposition. While this has proved to be effective in many instances, a detailed knowledge of airway geometry and pressure/flow inputs is required in order to accurately simulate particle deposition, in both healthy and diseased states. Often investigators resort to assumptions and simplifications, as these data are not readily available. These assumptions can drastically influence the results, reducing the ability of simulations to accurately reflect the real-world situation [3–5].

Two common simplifications for computational modeling of deposition are the use of a static airway structure and the assumptions of a uniform distribution of pressure or flow at the peripheral airways. Typically, the structural information on the airway tree is gained from computed tomography (CT) data during breath-holding [6–11].

Several of these studies have used changes in lobar volume measured from CT data at two points in the breathing cycle (e.g., functional residual capacity and total lung capacity) to estimate the flow division between lobes in order to formulate boundary conditions at the peripheral airways [6, 9, 10]. While an improvement over uniform pressure assumptions, this simplification does not take into account the dynamic flow effects throughout the respiratory cycle that result in variations in the distribution throughout the lung and also neglects intralobar variability.

Mead-Hunter *et al*. [3] studied the effect of the static airway structure simplification on deposition distributions calculated from numerical modeling. They found a significant difference in distributions when using a dynamic (moving) airway structure compared with those simulated using a static structure. This demonstrates the importance of including the dynamic airway geometry in deposition modeling and also highlights the sensitivity of deposition modeling to dynamic effects.

Measuring dynamic structural information for use in computational modeling of deposition represents an extremely useful capability. Furthermore, it is likely that dynamic regional ventilation measurements will allow more accurate boundary conditions to be formulated. A dynamic, functional lung imaging capability would, therefore, provide invaluable information for modeling studies, resulting in much improved deposition distribution simulations for study and optimization of delivery devices and particle sizes.

### 2.1.2 Regional Action of Delivered Drug

Lung function is spatially heterogeneous, and this heterogeneity is often increased when pathology is present. The lung has a great capacity to compensate when regions of the lung are diseased and underperforming. This compensation can mask disease when the loss of function is either subtle or highly patchy. Measurement of global lung function, such as using spirometry, provides an insensitive measure of function in these cases. While areas of the lung may be experiencing significant decreases in lung function, the total loss of function measured at the mouth may be negligible. Not only does this mask the progression of disease, but it may also not represent the true capacity for gas exchange with blood as it assumes matched heterogeneity of blood perfusion. The assessment of treatment outcomes through the global measurement of lung function is similarly insensitive. The capacity to measure regional functional information is essential for sensitive assessment of a treatment's performance and viability for the development of drugs and delivery mechanisms.

Although imaging can provide sensitive information for assessment of a treatment's performance, it is underutilized in pharmaceutical development, with only about 1% or 2% of animals used in the preclinical stages of drug development receiving an imaging measurement [1]. The development and widespread utilization of truly functional imaging measurements for the lung has a capacity to enhance decision making in the development of pulmonary drugs and drug delivery methods, and also offers the potential to be a major influence on the treatment through the personalization of these factors.

### 2.1.3 The Role of Functional Lung Imaging in Pulmonary Drug Delivery

Functional lung imaging can help to attack key challenges in the advancement of pulmonary drug delivery, by providing regional function information. Imaging technologies that are capable of measuring airflow and other functional parameters within the breathing lung can provide information critical to the understanding of the delivery of particles and aerosols under both normal and pathological conditions. Furthermore, functional lung imaging offers the regional measurement of treatment efficacy, a capability that is crucial for investigating the interplay between airflow, particle/aerosol deposition, and improved functional outcomes.

The respiratory system offers unique challenges for imaging. The lung contains a complicated branching geometry, with a structure that contains functional elements across a wide range of scales (Chapter 1). Furthermore, the respiratory system is dynamic, with complicated movement that is intimately linked to function [12].

The ideal functional imaging method would contain three specific characteristics: noninvasiveness, high spatial resolution, and capability for dynamic measurements.

A. *Noninvasiveness*. The ability to perform measurements in a noninvasive manner is critical for probing any biological system. The processes in the lung involve complicated interactions of chemical, physiological, and mechanical factors. Disruption of any of these factors may result in a misrepresentation of the process being investigated. The noninvasive measurement of lung function requires imaging through opaque tissue, which eliminates visible light modes of imaging such as microscopy from being used. Ideally, imaging of lung function will be performed without the introduction of contrast agents, as these can disturb both the physical and chemical interactions within the lung.
B. *Spatial resolution*. The lung is a complicated system, with important interactions occurring across multiple scales. For example, the flow of air through the trachea and other major airways is a critical factor for airway deposition. The size of the trachea and that of the major airways in humans are in the centimeter range. In contrast, the alveoli in the mammalian lungs range in size from 80 μm in mice to 210 μm in humans [13]. The functionally important heterogeneity in the lung occurs between these scales, and, therefore, high-resolution imaging is required to capture the regional distribution of functional changes within the lung.

C. *Dynamic measurement*. Normal human respiration is dynamic and periodic. The process of breathing causes time-varying changes in the tissue structure and airway geometry. These dynamic factors are important indicators in most lung pathologies. For example, asthma is a disease that acts to restrict the airway caliber causing an increase in airway resistance with a subsequent reduction in the peak expiratory flow. Common treatments for asthma are inhaled airway dilators that counteract this constriction to increase the peak expiratory flow. Static imaging or imaging between two static breath-hold states can only capture the structural changes that occur in asthma, that is, the changes in airway caliber. Dynamic measurements are necessary to measure the functional consequences of these structural changes, i.e., the peak flows. An additional factor to consider is the time scale over which the effects of treatments for lung disease occur. Treatments with transient or short-lived effects require dynamic measurements of function to accurately assess their efficacy.

In this chapter, both established and emerging technologies for functional lung imaging have been reviewed, and these have been discussed in the context of pulmonary drug delivery. The role that functional imaging can play in improving our understanding of particle/aerosol deposition and in the development of drug delivery systems has been considered. The potential of functional imaging as a tool for the improvement of pulmonary drug delivery has been demonstrated, and the possibilities for patient-specific tailoring of pulmonary drug delivery parameters have been explored. The overall aim is to encourage the use of functional lung imaging in pulmonary drug delivery development and stimulate the development of functional lung imaging technologies to better address the requirements in this field.

## 2.2 Established Functional Lung Imaging Technologies

Several modes of lung imaging are well established. In this section, we provide an overview, explain the technical principles and describe the advantages and disadvantages of each technology. Our goal is to provide a working knowledge of the capabilities of each imaging mode to allow researchers to assess their possible use in the context of pulmonary drug delivery development.

### 2.2.1 Computed Tomography

CT is currently the best practice for lung imaging. CT is an X-ray-based imaging method, whereby images are acquired from multiple viewing angles to provide projections or line integrals of the sample from different angular orientation. These projections are then combined using back-projection or iterative methods to form a three-dimensional (3D) image of the lung. The spatial resolution of the reconstruction is dependent on both the spatial resolution of the projections and the number of viewing angles used in the reconstruction. A high-resolution CT scan requires many high-resolution projection images to be acquired.

Almost all clinical CT machines employ a single source and detector pair, which is rotated around the patient to collect the projection data. Artifacts will be present in the reconstructions if the object is not in the same position during the acquisition of each projection or it moves in between projection acquisitions. Therefore, traditional CT can only be performed on a stationary object. This typically requires the patient to perform a breath-hold maneuver to avoid artifacts in lung CT. Additionally, treatments with short-lived effects that occur on a time scale that is shorter than the scan time (typically many minutes) cannot be captured.

CT is an X-ray-based imaging method, and, therefore, the radiation dose is of a significant concern. The ionizing nature of absorbed X-rays can damage DNA, either directly or through the creation of free radicals. For this reason, X-ray exposure (also known as dose) significantly increases the probability of developing cancerous tumors. Therefore, it is necessary to minimize the radiation dose

in any X-ray imaging method, particularly in CT where the use of many projection images results in high radiation exposure [14]. The requirement for minimization of dose means that it is difficult to perform longitudinal studies to investigate lung disease progression, or to monitor the effectiveness of certain treatments over time.

CT has the ability to provide measurement of lung health under a variety of conditions. For example, Galbán *et al*. [15] used changes between two CT reconstructions (one at end inspiration and another at end expiration) as a surrogate biomarker for chronic obstructive pulmonary disease. Using this method, they were able to assess the regional severity of the disease. De Langhe *et al*. [16] quantified lung fibrosis and emphysema in mice using CT which can be utilized to provide either an indirect assessment of lung health through biomarkers or a direct measurement of lung health where structural changes in lung tissue can be resolved. Unfortunately, many lung diseases may produce large functional changes for only subtle changes in the lung structure that may not be readily deduced from static CT imaging, until or unless the effect becomes large.

### 2.2.2 Ventilation Measurement using 4DCT Registration-based Methods

The movement of air through the lungs is affected by the diaphragm and chest-wall muscles, resulting in expansion and contraction of the alveoli and displacement of lung tissue. The motion of lung tissue is, therefore, integrally connected to its function, and measurement of lung tissue expansion allows inference of flow into and out of the specific lung regions.

CT has been combined with image registration techniques to provide the measurement of lung motion. Image registration was originally developed to match the spatial location of images of static objects which had moved due to natural misalignments in the imaging system or that of the object. However, this process can also be used to measure the displacement of objects between images. Several studies have used image registration to measure the motion of the lung tissue between two volumetric lung images acquired using CT in two breath-hold states [17–20]. Unfortunately, data measured in this way do not truly capture the dynamics of breathing.

An alternative method is to exploit the periodic motion of the lung during the breathing cycle to perform phase matching of projection data, allowing phase-averaged four-dimensional computed tomography (4DCT) of the lung to be performed at various points in the breathing cycle. Several studies have combined this method with image registration to measure lung motion and regional ventilation during the breathing cycle [21–23]. These data can be used to assess the health of the lung tissue. For example, this technique was demonstrated to measure regional disease in patients with emphysema [24].

Despite being a very powerful tool for regional lung function assessment, the 4DCT-based measurement of ventilation requires at least one additional CT scan to be acquired for each time-point measured. This exposes the subject to a very high radiation dose that makes serial imaging impractical and limits its use to subjects where significant risks of large radiation dose are acceptable, for example, patients with advanced disease or preclinical models. Furthermore, as the measurements are averaged over many breaths, short-lived or transient effects cannot be captured using this method.

### 2.2.3 Hyperpolarized Magnetic Resonance Imaging

Magnetic resonance imaging (MRI) detects the radio-frequency (RF) signals emitted by polar nuclei when their spin is modified by an external magnetic field. Hydrogen atoms abound in biological tissue, and this has been the traditional target element used to image soft tissue with MRI. However, the low tissue density within the lung (since the inflated lung is approximately 80% air) results in very poor image quality. To overcome this problem, hyperpolarized noble gases have been produced, which when inhaled enhance the MRI signal from the lung by several orders of magnitude. Additionally, as the signal is proportional to the concentration of the gas, regional variation in the

ventilation distribution may be obtained [25]. By utilizing specialized magnetizing sequences, other functional measurements may be performed such as lung microstructure, oxygenation, and perfusion [26], although with varying degrees of success.

A major advantage of hyperpolarized MRI over CT is the ability to obtain an image without imparting radiation dose. However, despite recent improvements, the resolution is still significantly lower than CT.

Despite its potential and recent advances, there exist a number of challenges hindering a widespread use of hyperpolarized MRI [26]. Cost is the most significant factor. Highly specialized and expensive technology is required to produce the necessary magnetic field for imaging the hyperpolarized gas. Furthermore, the production of the hyperpolarized gases is also expensive, and the limited half-life of such gases causes availability and logistical issues [27]. Perhaps due to the prohibitive cost of hyperpolarized MRI, no substantial study has yet demonstrated the relative sensitivity and specificity advantages of this method over other modalities.

### 2.2.4 Electrical Impedance Tomography

The chest cavity consists mainly of blood, tissue, and air, and the proportions of these materials in the chest will vary over the respiratory and cardiac cycles. The electrical resistivity and impedance of regions within the body vary depending on the proportions of the various constituents. Electrical impedance tomography (EIT) exploits this to measure the changes in ventilation and perfusion during breathing. The different electrical properties of blood, tissue, and air can be used to determine the regional ventilation and blood perfusion within the lungs [28–30]. Electrodes are placed around the chest, and voltage profiles are collected for all drive and receive electrode–pair combinations. These data are are tomographically reconstructed to map the time-varying electrical properties within the lungs during breathing. This method is noninvasive and, with a temporal resolution of around 33 Hz [29], is adequate for dynamic lung studies. Additionally, due to the relatively simple and compact hardware requirement, EIT can be performed at the bedside, which is clearly advantageous for clinical applications. However, spatial resolution is fundamentally limited and is much lower than the CT- or MRI-based modalities. This is due, in part, to the ill-posed problem of the reconstruction, resulting from limitations on the maximum number of electrode/detector pairs [28] that can practically be used. Additionally, the electrical currents induced by the electrodes typically flow outside of the electrode plane (up to 10 cm) [30], reducing spatial resolution even further.

EIT can provide assessment of lung health, making it useful as a clinical tool for monitoring patients. However, for pulmonary drug delivery development, where smaller scale regional function changes are important, the lack of spatial resolution limits the utility of EIT.

### 2.2.5 Nuclear Medical Imaging (PET/SPECT)

The category of nuclear medical imaging methods contains three major imaging modes: gamma scintigraphy, positron emission tomography (PET), and single-photon emission computed tomography (SPECT). These modalities utilize the detection of gamma-ray photons emitted from within a subject by a pharmaceutical compound labeled with a radioactive isotope. The radio-labeled substance is used to preferentially target an organ or disease process.

Gamma scintigraphy is a planar method, where the emitted gamma-rays are collimated and collected by a photon-counting detector, enabling a two-dimensional view of the concentration of radionuclide in the subject. PET and SPECT utilize a similar imaging principle, whereby measurements from various viewing angles are tomographically reconstructed in order to produce a three-dimensional image.

Although localization of the labeled pharmaceutical compound to specific areas can provide excellent contrast, nuclear medicine techniques generally suffer from a poor signal-to-noise ratio as the

amount of radioactive material must be minimized for the safety of the subject. Although spatial resolutions have improved dramatically over the past decade, temporal resolution remains poor [31].

Nuclear medicine enables studies of lung function to be carried out, including the determination of regional ventilation and gas exchange [32–34]. For functional lung imaging, this radioactive agent is inhaled into the lungs. Functional lung measurements using nuclear imaging are well suited for testing the efficacy of pulmonary drug delivery to provide a measure of a treatment success from a functional, as opposed to anatomical, perspective. Additionally, the functional data obtained may be used as a validation for numerical simulation [6].

Radionuclide agents can be tagged to specific materials, and consequently nuclear imaging can be used to directly track deposition of pharmaceutical compounds into the lung – a highly useful tool for pulmonary drug delivery development [2]. This allows measurement of deposition patterns for specific delivery methods and when combined with functional imaging enables drug deposition to be correlated with global functional response, as well as providing data for validation of deposition models. PET imaging provides the best regionality and resolution for this purpose; however, practical challenges limit its widespread use, such as difficulties in producing radiolabeled drug analogues and the very short half-lives of suitable radionuclides [35].

## 2.3 Emerging Technologies

As is apparent from the above, several imaging technologies have been used for lung imaging, with various advantages and disadvantages. However, there is a need for further advancements to address the key shortfalls of the current technology for providing the ideal functional lung imaging capability. The key will be to deliver functional imaging with sufficient resolution and contrast in the lung while maintaining a dynamic imaging capability. Over the last decade, synchrotron-based phase-contrast imaging methods have made huge advances toward this goal. The unique properties of synchrotron radiation are advantageous for imaging the lung, and translation of these techniques to laboratory-based X-ray sources, and eventually to clinical application promises to provide lung-imaging modalities with unprecedented capabilities.

In this section, we describe synchrotron-based phase-contrast imaging and give examples of its use in the lung. Recent efforts in the translation of these technologies to laboratory-based systems are then detailed.

### 2.3.1 Phase-contrast Imaging

X-ray imaging traditionally utilizes absorption contrast, whereby materials with differing X-ray attenuation properties are differentiated by the intensity of the X-rays that pass through it. A structure that contains a heavily attenuating material will appear darker than that containing a less attenuating material. For example, as bone is much more attenuating than the surrounding soft tissue, it provides a highly contrasting structure. Conversely, the lung parenchyma and surrounding tissue have similar bulk attenuation properties, and, therefore, the lungs generate poor contrast.

Phase-contrast imaging utilizes the difference in refractive properties of materials to generate contrast. In a manner similar to holography, differential changes in the phase of a partially coherent X-ray wave, imparted by different materials in the sample, can be made visible as a consequence of interference with an unperturbed wave. Since the phase gradients are greatest at the boundaries between materials, phase contrast has a predominantly edge-enhancing effect.

For phase-contrast imaging, an X-ray source with high spatial and temporal coherence is ideally required. The extreme brightness of synchrotron radiation sources enables the conditioning of the X-ray beam to create very high coherence while maintaining sufficient flux to image within reasonable temporal resolution. Specifically, the X-ray energy can be filtered to produce a monochromatic beam

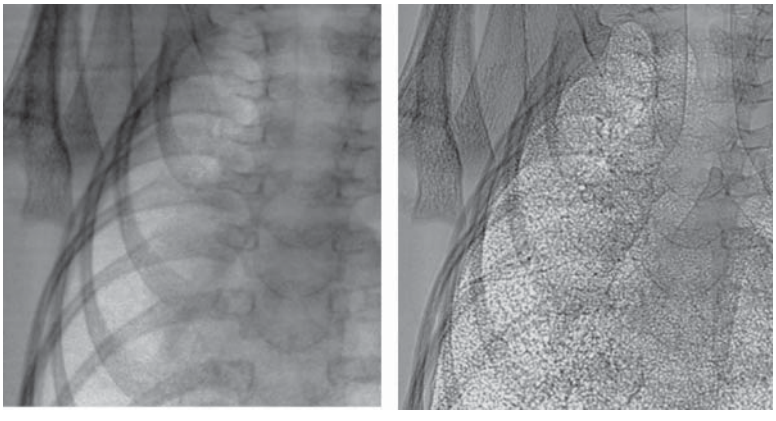

***Figure 2.2*** *Synchrotron phase-contrast imaging of a newborn rabbit pup lung. Propagation-based phase–contrast images acquired using monochromatic synchrotron radiation (right) provides enhanced detail of the fine structures of the lung when compared to absorption-based imaging (left). Significantly more detail of the lung is visible in the phase-contrast image. Images were acquired at the BL20B2 beamline at the SPring-8 Synchrotron, Japan (See insert for color representation of this figure)*

to improve temporal coherence, while the distance from the X-ray source to the sample can be increased to reduce the effective spot size and increase spatial coherence [31]. Notwithstanding the dramatic advantages for phase-contrast imaging, synchrotron radiation sources are highly expensive, requiring specialized facilities, and consequently access to these X-ray sources is limited. In order to become widely adopted, the phase-contrast imaging technologies developed on the synchrotron must be translated into the laboratory, and ultimately to a clinical setting. Recent developments toward this initial translation to laboratory-sized X-ray sources have generated promising results, and widespread laboratory-based phase-contrast imaging is now within reach.

There has been considerable effort over the last decade to develop phase-contrast imaging for the lung. The air/tissue interfaces in the lung provide very large X-ray phase gradients; phase-contrast imaging is ideally suited for lung imaging, providing significant improvements in contrast and detail over absorption-based X-ray imaging (Figure 2.2).

Several methods for generating phase contrast have been applied to the lung, with the two most predominant being grating interferometry and propagation-based imaging (PBI).

### 2.3.2 Grating Interferometry

Grating interferometry [36, 37] uses phase gratings placed between the sample and detector to generate contrast from the phase changes imparted on the X-ray wave by the sample. As the gratings are placed between the detector and sample, there is an effective decrease in the efficiency of the system to detect X-rays. This necessitates either very bright X-ray sources, or increased exposure times, subsequently resulting in a relative increase in the X-ray dose imparted to the sample.

These methods are well suited to X-ray sources that exhibit lower coherence. Consequently, although initially developed using synchrotron radiation sources, there have been several recent studies using grating interferometry on a laboratory-based X-ray source [38] with several recent studies relating to lung imaging [39–41].

Schwab *et al*. [41] used a compact laboratory-based synchrotron to demonstrate improved contrast in excised healthy mouse lungs using grating-based imaging. This same imaging setup was also used by Schleede *et al*. [40] to demonstrate improved diagnosis of emphysema by comparing the ratio of the phase signal to the attenuation signal, a surrogate marker for alveolar size.

Meinel *et al*. [39] attempted to use a similar measure on the same setup for the improvement of lung cancer detection. The preliminary results did not show any increase in sensitivity; however, the delineation of the cancer boundary was improved through the edge-enhancing effect.

Grating interferometry shows the potential for use in assessing the effectiveness of drug delivery treatments. However, although this approach is potentially more sensitive in some cases, the data obtained are structural and, thus, can only provide anatomical markers for treatment efficacy rather than produce functional markers.

Furthermore, until temporal resolution is improved, dynamic measurements will not be possible, further limiting its utility.

### 2.3.3 Propagation-based Phase-contrast Imaging

Propagation-based phase-contrast imaging (PBI), sometimes called in-line X-ray phase-contrast imaging, is by far the simplest method for generating phase contrast. By allowing the X-ray wave to propagate a large distance between the sample and detector, the X-ray waves that are slightly refracted at the surface interface interfere at the detector plane to generate intensity fringes. The ability to image in phase contrast without gratings or other apparatus between the sample and detector provides a higher efficiency and, therefore, increased capability for dynamic imaging [42]. Due to its simple implementation, and capacity for dynamic imaging, there are a number of studies that have utilized planar PBI for *in vivo* lung imaging. For example, Hooper *et al*. [43] visualized liquid clearance in live newborn rabbit pups as they take their first breaths. Kitchen *et al*. [44] described a method for calculating ventilation from dynamic imaging of lungs using PBI, demonstrating the possibility for functional metrics to be derived from phase-contrast images.

The use of dynamic PBI for investigations into drug delivery has been demonstrated in several recent studies, and development of image processing and experimental methods stemming from this core technology has accelerated in recent years, with applications to various diseases and/or drug delivery models. Donnelley *et al*. [45] demonstrated detection of inhalable particles in live mouse airways using high-resolution synchrotron PBI. Subsequent to this, the pollutant and other marker particles were used to measure mucociliary transport mechanisms [46]. This may have utility in assessing treatments for diseases that affect the mucociliary transport system. Morgan *et al*. [47] used PBI to measure airway surface liquid depth, specifically for the assessment of therapies for cystic fibrosis lung disease. Donnelley *et al*. [48] measured the variability of the *in vivo* fluid dose distribution in liquid doses delivered through the pulmonary system. These studies have exploited the dynamic capabilities of synchrotron PBI in order to probe both the effectiveness of treatments and the efficacy of the delivery methods.

### 2.3.4 Functional Lung Imaging using Phase Contrast

The increased spatial detail and temporal resolution resulting from PBI of the lung provide the opportunity for advanced image processing methods to extract quantitative functional information for diagnosis and assessment of disease.

Motion-tracking methods, originally developed to measure fluid flow in engineering applications, have been adapted to measure the motion of lung tissue in dynamic PBI images [49]. The motion and expansion of the lung tissue are directly linked to the airflow into, or out of, regions of the lung, so these motion fields can be used to calculate airflow distributions throughout the lung [50], thus adding a functional measurement capability.

Fouras *et al*. [49] demonstrated that the motion of the lung tissue can be used as a biomarker for lung injury, providing improved sensitivity and earlier detection of disease over other methods.

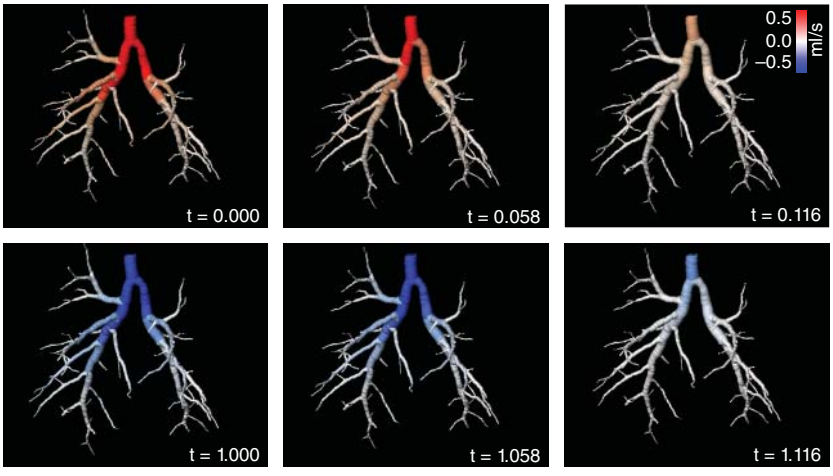


***Figure 2.3*** *Distribution of flow throughout the airway tree, measured using functional lung imaging (Source: Reproduced with permission from [50]) (See insert for color representation of this figure)*

Dubsky *et al*. [50] developed a method for 4D dynamic measurements of airflow throughout the entire lung (Figure 2.3). This method can, thus, provide both the functional assessment of treatments and high-quality inputs for computational modeling. The application of this functional imaging method to the assessment of cystic fibrosis lung disease demonstrated a large improvement in sensitivity and accuracy. This method is based on 4DCT, and, therefore, imparts significant dose to the subject. However, our research group has also developed a novel method that can reduce the dose by orders of magnitudes, allowing the 4D measurement of lung motion from as few as six images [51–53]. This method can also provide the dynamic measurement of short-lived effects, significantly broadening the scope of treatments and conditions that can be assessed, particularly for investigations into inhaled treatments for which the functional effects are often transient.

Instantaneous flow of air through the rabbit pup airway tree at six time points (from the sequence of 20 time points) during ventilation. The positive flow (red) indicates the inspiratory flow and the negative flow (blue) indicates the expiratory flow.

Functional lung imaging using phase contrast has been demonstrated to outperform any current imaging methods for assessment of disease and treatments. However, the requirement for synchrotron radiation severely limits its widespread adoption. In order to fully realize the potential in this field, the technology must be translated from the synchrotron to the laboratory, and then into the clinic.

### 2.3.5 Laboratory Propagation-based Phase-contrast Imaging

It was demonstrated almost 20 years ago that PBI could be performed on a laboratory source with sufficient spatial coherence [54]. Only recently, the X-ray source technology has enabled this method to be used with sufficient temporal resolution to be useful for lung imaging. The challenge lies in creating an X-ray source with adequate power and a source spot size small enough to deliver the required spatial coherence.

Garson *et al*. [55] demonstrated that lung images of similar quality to those acquired at a synchrotron can be produced using laboratory-based sources; however, the standard X-ray source used resulted in exposure times that are too long for dynamic or *in vivo* studies.

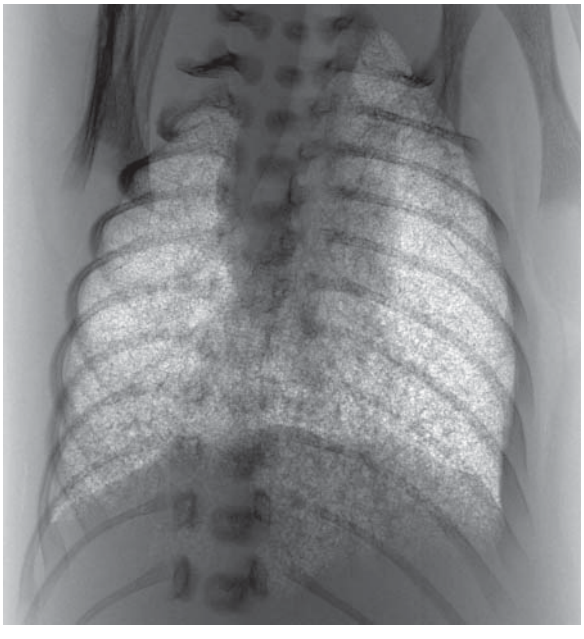

***Figure 2.4*** *Laboratory propagation-based phase-contrast imaging. Image of a newborn rabbit pup lung acquired on a liquid-metal-jet laboratory X-ray source. The image quality is comparable to synchrotron-based phase-contrast imaging demonstrating the viability of the translation of phase-contrast imaging techniques to the laboratory and ultimately the clinic*

With the recent development of liquid-metal-jet X-ray sources, the possibility for dynamic PBI in the laboratory has emerged. The liquid-metal-jet X-ray source provides unparalleled brightness for small spot sizes, allowing for very high quality phase-contrast imaging with reduced exposure times [56]. PBI using the liquid-metal-jet source has been demonstrated in a number of applications, including for high-resolution angiography [57] and cancer detection/demarcation in small animals [58].

It has recently been demonstrated that successful high-resolution dynamic phase-contrast *in vivo* lung imaging (Figure 2.4) can be affected using a liquid-metal-jet laboratory X-ray source (Excillum, D2). Using this new technology, the translation of functional dynamic phase-contrast imaging from the synchrotron to the laboratory is a viable option, and the full potential of these methods are likely to be realized in the near future.

## 2.4 Conclusion

This chapter has described the established and cutting-edge lung imaging technologies, and outlined their possible applications for improving the development of pulmonary drug delivery treatments. Two major areas of involvement are envisaged: assessment of treatment efficacy and creating experimental input data for simulations.

Significant values will be added through new functional imaging technologies. Functional biomarkers predominantly respond much earlier to changes in disease states than anatomical biomarkers, and so functional imaging has the capacity to accelerate the development pipeline dramatically. In another

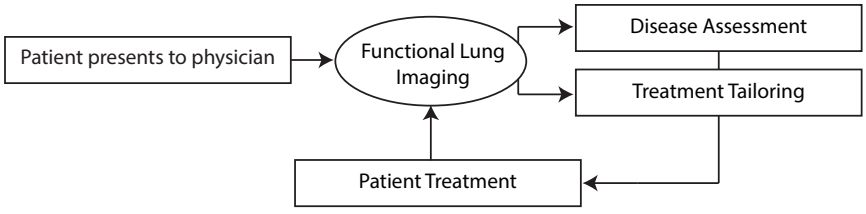


***Figure 2.5*** *Integration of functional lung imaging with pulmonary drug delivery treatment*

aspect, functional data provide more complete and accurate inputs for deposition simulations, further improving the use of these in drug delivery development.

The key challenges for fully realizing this potential will be providing broad access to functional imaging technologies for researchers in the field of pulmonary drug delivery. The most exciting technologies are being incubated at synchrotron imaging facilities, and translation of these into the laboratory, and ultimately the clinic, will be critical. Progress toward this goal is accelerating.

Functional lung imaging can provide diagnosis, inputs for optimization of drug delivery parameters, and treatment monitoring. This can provide improved patient outcomes in the treatment of lung disease.

While contributing to pulmonary drug delivery development promises to add a huge amount of value, there also exists the potential for functional lung imaging to become core to the treatment process itself. An example scenario is described in Figure 2.5. In this scenario, lung imaging is used for three purposes. First, imaging is used to diagnose and assess the severity of the pathology that is present in the patient. Second, data from functional imaging are used as inputs into patient-specific deposition simulations, allowing tailoring of the inhaled treatment parameters to the specific status of the patient. Third, functional imaging is used to monitor the effectiveness of the treatment, and potentially adapt the treatment to the changing condition of the patient. Future advances in dose reduction and quality of outputs will allow the full integration of functional lung imaging into the pulmonary drug delivery treatment process, with the potential to dramatically improve efficiency and effectiveness of treatments, leading to improved patient outcomes.

## References

1. Ricketts S.-A., Hockings P.D., Waterton J.C. (2011). Non-invasive imaging in the pharmaceutical industry. Berlin: Springer. pp. 17–27.
2. Conway J. (2012). Lung imaging – two dimensional gamma scintigraphy, spect, CT and PET. *Advanced Drug Delivery Reviews*, **64**, 357–368.
3. Mead-Hunter R., King A.J.C., Larcombe A.N., Mullins B.J. (2013). The influence of moving walls on respiratory aerosol deposition modelling. *Journal of Aerosol Science*, **64**, 48–59.
4. Wall W.A., Rabczuk T. (2008). Fluid–structure interaction in lower airways of CT-based lung geometries. *International Journal for Numerical Methods in Fluids*, **57**(5), 653–675.
5. Xia G., Tawhai M.H., Hoffman E.A., Lin C.-L. (2010). Airway wall stiffening increases peak wall shear stress: A fluid–structure interaction study in rigid and compliant airways. *Annals of Biomedical Engineering*, **38**(5), 1836–1853.
6. De Backer J.W. Vos W.G., Vinchurkar S.C., *et al*. (2010). Validation of computational fluid dynamics in ct-based airway models with spect/ct. *Radiology*, **257**(3), 854-862.
7. De Backer W. Devolder A., Poli G., *et al*. (2010). Lung deposition of BDP/formoterol HFA pMDI in healthy volunteers, asthmatic, and copd patients. *Journal of Aerosol Medicine and Pulmonary Drug Delivery*, **23**(3), 137–148.

8. Inthavong K. Choi L.-T., Tu J., *et al*. (2010). Micron particle deposition in a tracheobronchial airway model under different breathing conditions. *Medical Engineering and Physics*, **32**(10), 1198–1212.
9. Lambert A.R. O'Shaughnessy P.T., Tawhai M.H., *et al*. (2011). Regional deposition of particles in an image-based airway model: Large-eddy simulation and left–right lung ventilation asymmetry. *Aerosol Science and Technology*, **45**(1), 11–25.
10. Vinchurkar S. De Backer L., Vos W., *et al*. (2012). A case series on lung deposition analysis of inhaled medication using functional imaging based computational fluid dynamics in asthmatic patients: Effect of upper airway morphology and comparison with in vivodata. *Inhalation Toxicology*, **24**(2), 81–88.
11. Xiong T. (2012). Flow and particles deposition in anatomically realistic airways. *Computer Methods in Biomechanics and Biomedical Engineering*, **15**(Suppl. 1), 56–58.
12. Weibel E.R. (2009). What makes a good lung? *Swiss Medical Weekly*, **139**(27–28), 375–386.
13. Irvin C.G., Bates J.H.T. (2003). Measuring the lung function in the mouse: The challenge of size. *Respiratory Research*, **4**, 4.
14. Brenner D.J., Hall E.J. (2007). Current concepts – computed tomography – an increasing source of radiation exposure. *New England Journal of Medicine*, **357**(22), 2277–2284.
15. Galbán C.J. (2012). Computed tomography-based biomarker provides unique signature for diagnosis of copd phenotypes and disease progression. *Nature Medicine*, **18**(11), 1711–1715.
16. De Langhe E. VandeVelde G., Hostens J., *et al*. (2012). Quantification of lung fibrosis and emphysema in mice using automated micro-computed tomography. *Plos One*, **7**(8), e43123.
17. Christensen G.E. Song J.H., Lu W., *et al*. (2007). Tracking lung tissue motion and expansion/compression with inverse consistent image registration and spirometry. *Medical Physics*, **34**(6), 2155–2163.
18. Ding K. Bayouth J.E., Buatti J.M., *et al*. (2010). 4DCT-based measurement of changes in pulmonary function following a course of radiation therapy. *Medical Physics*, **37**(3), 1261–1272.
19. Reinhardt J.M. Ding K., Cao K., *et al*. (2008). Registration-based estimates of local lung tissue expansion compared to xenon CT measures of specific ventilation. *Medical Image Analysis*, **12**(6), 752–763.
20. Yin Y. Choi J., Hoffman E.A., et al. (2010). Simulation of pulmonary air flow with a subject-specific boundary condition. *Journal of Biomechanics*, **43**(11), 2159–2163.
21. Castillo R., Castillo E., Martinez J., Guerrero T. (2010). Ventilation from four-dimensional computed tomography: Density versus Jacobian methods. *Physics in Medicine and Biology*, **55**(16), 4661–4685.
22. Guerrero T. Sanders K., Castillo E., *et al*. (2006). Dynamic ventilation imaging from four-dimensional computed tomography. *Physics in Medicine and Biology*, **51**(4), 777–791.
23. Pan T., Lee T.-Y., Rietzel E., Chen G.T.Y. (2004). 4DCT imaging of a volume influenced by respiratory motion on multi-slice CT. *Medical Physics*, **31**(2), 333–340.
24. Yamamoto T. Kabus S., Klinder T., *et al*. (2011). Investigation of four-dimensional computed tomography-based pulmonary ventilation imaging in patients with emphysematous lung regions. *Physics in Medicine and Biology*, **56**(7), 2279–2298.
25. Ebert M. Grossmann T., Heil W., *et al*. (1996). Nuclear magnetic resonance imaging with hyperpolarised helium-3. *Lancet*, **347**(9011), 1297–1299.
26. Emami K. Stephen M., Kadlecek S., *et al*. (2009). Quantitative assessment of lung using hyperpolarized magnetic resonance imaging. *Proceedings of the American Thoracic Society*, **6**(5), 431–438.
27. Dunster K.R. Friese M.E.J., Fraser J.F., *et al*. (2012). Ventilation distribution in rats: Part 2 – a comparison of electrical impedance tomography and hyperpolarised helium magnetic resonance imaging. *Biomedical Engineering Online*, **11**, 68.

28. Cheney M., Isaacson D., Newell J.C. (1999). Electrical impedance tomography. *SIAM Review*, **41**(1), 85–101.
29. Frerichs I. (2000). Electrical impedance tomography (EIT) in applications related to lung and ventilation: A review of experimental and clinical activities. *Physiological Measurement*, **21**(2), R1–R21.
30. Victorino J. Borges J., Okamoto V., *et al*. (2004). Imbalances in regional lung ventilation – A validation study on electrical impedance tomography. *American Journal of Respiratory and Critical Care Medicine*, **169**(7), 791–800.
31. Fouras A. Kitchen M.J., Dubsky S., *et al*. (2009). The past, present, and future of x-ray technology for in vivo imaging of function and form. *Journal of Applied Physics*, **105**(10), 102009.
32. Musch G. Layfield J., Harris R., *et al*. (2002). Topographical distribution of pulmonary perfusion and ventilation, assessed by pet in supine and prone humans. *Journal of Applied Physiology*, **93**(5), 1841–1851.
33. Harris R.S., Schuster D.P. (2006). Visualizing lung function with positron emission tomography. *Journal of Applied Physiology*, **102**(1), 448–458.
34. Jobse B.N. Rhem R.G., McCurry C.A.J.R., *et al*. (2012). Imaging lung function in mice using SPECT/CT and per-voxel analysis. *Plos One*, **7**(8), e42187.
35. Newman S., Fleming J. (2011). Challenges in assessing regional distribution of inhaled drug in the human lungs. *Expert Opinion on Drug Delivery*, **8**(7), 841–855.
36. Weitkamp T. Diaz A., David C., *et al*. (2005). X-ray phase imaging with a grating interferometer. *Optics Express*, **13**(16), 6296–6304.
37. Zhu P. Zhang K., Wang Z., *et al*. (2010). Low-dose, simple, and fast grating-based x-ray phase-contrast imaging. *Proceedings of the National Academy of Sciences*, **107**(31), 13576–13581.
38. Tapfer A. Bech M., Velroyen A., *et al*. (2012). Experimental results from a preclinical x-ray phase-contrast CT scanner. *Proceedings of the National Academy of Sciences*, **109**(39), 15691–15696.
39. Meinel F.G. Schwab F., Yaroshenko A., *et al*. (2013). Lung tumors on multimodal radiographs derived from grating-based x-ray imaging – a feasibility study. *Physica Medica*, **30**(3), 352–357.
40. Schleede S. Meinel F.G., Bech M., *et al*. (2012). Emphysema diagnosis using x-ray dark-field imaging at a laser-driven compact synchrotron light source. *Proceedings of the National Academy of Sciences*, **109**(44), 17880–17885.
41. Schwab F. Schleede S., Hahn D., *et al*. (2013). Comparison of contrast-to-noise ratios of transmission and dark-field signal in grating-based x-ray imaging for healthy murine lung tissue. *Zeitschrift fur Medizinische Physik*, **23**(3), 236–242.
42. Lewis R. Yagi N., Kitchen M., *et al*. (2005). Dynamic imaging of the lungs using x-ray phase contrast. *Physics in Medicine and Biology*, **50**(21), 5031–5040.
43. Hooper S.B. Kitchen M.J., Siew M.L., *et al*. (2009). Imaging lung aeration and lung liquid clearance at birth using phase contrast x-ray imaging. *Clinical and Experimental Pharmacology and Physiology*, **36**(1), 117–125.
44. Kitchen M.J. Lewis R.A., Morgan M.J., *et al*. (2008). Dynamic measures of regional lung air volume using phase contrast x-ray imaging. *Physics in Medicine and Biology*, **53**(21), 6065–6077.
45. Donnelley M. Morgan K.S., Fouras A., *et al*. (2009). Real-time non-invasive detection of inhalable particulates delivered into live mouse airways. *Journal of Synchrotron Radiation*, **16**(4), 553–561.
46. Donnelley M., Morgan K.S., Siu K.K.W., Parsons D.W. (2012). Dry deposition of pollutant and marker particles onto live mouse airway surfaces enhances monitoring of individual particle mucociliary transit behaviour. *Journal of Synchrotron Radiation*, **19**(Pt 4), 551–558.
47. Morgan K.S. Donnelley M., Paganin D.M., *et al*. (2013). Measuring airway surface liquid depth in ex vivo mouse airways by x-ray imaging for the assessment of cystic fibrosis airway therapies. *Plos One*, **8**(1), e55822.

48. Donnelley M., Morgan K.S., Siu K.K.W., Parsons D.W. (2013). Variability of in vivo fluid dose distribution in mouse airways is visualized by high-speed synchrotron x-ray imaging. *Journal of Aerosol Medicine and Pulmonary Drug Delivery*, **26**(5), 307–316.
49. Fouras A. Allison B.J., Kitchen M.J., *et al*. (2012). Altered lung motion is a sensitive indicator of regional lung disease. *Annals of Biomedical Engineering*, **40**(5), 1160–1169.
50. Dubsky S., Hooper S.B., Siu K.K.W., Fouras A. (2012). Synchrotron-based dynamic computed tomography of tissue motion for regional lung function measurement. *Journal of the Royal Society Interface*, **9**(74), 2213–2224.
51. Dubsky S., Hooper S.B., Siu K. (2012). In vivo tomographic velocimetry of the lung for the detailed study of lung disease and its treatments. *Proceedings of SPIE Optical* **8506**.
52. Dubsky S. Jamison R.A., Higgins S.P.A., *et al*. (2010). Computed tomographic x-ray velocimetry for simultaneous 3d measurement of velocity and geometry in opaque vessels. *Experiments in Fluids*, **52**(3), 543–554.
53. Dubsky S. Jamison R.A., Irvine S.C., *et al*. (2010). Computed tomographic x-ray velocimetry. *Applied Physics Letters*, **96**(2), 023702.
54. Wilkins S.W. Gureyev T.E., Gao D., *et al*. (1996). Phase-contrast imaging using polychromatic hard x-rays. *Nature*, **384**(6607), 335–338.
55. Garson A.B., III, Izaguirre E.W., Price S.G., Anastasio M.A. (2013). Characterization of speckle in lung images acquired with a benchtop in-line x-ray phase-contrast system. *Physics in Medicine and Biology*, **58**(12), 4237–4253.
56. Tuohimaa T., Otendal M., Hertz H.M. (2007). Phase-contrast x-ray imaging with a liquid-metal-jet-anode microfocus source. *Applied Physics Letters*, **91**(7), 074104.
57. Lundström U. Larsson D.H., Burvall A., *et al*. (2012). X-ray phase contrast for $CO_2$ microangiography. *Physics in Medicine and Biology*, **57**(9), 2603–2617.
58. Larsson D.H. Lundström U., Westermark U.K., *et al*. (2013). First application of liquid-metal-jet sources for small-animal imaging: High-resolution CT and phase-contrast tumor demarcation. *Medical Physics*, **40**(2), 021909.